



저작자표시-비영리-변경금지 2.0 대한민국

이용자는 아래의 조건을 따르는 경우에 한하여 자유롭게

- 이 저작물을 복제, 배포, 전송, 전시, 공연 및 방송할 수 있습니다.

다음과 같은 조건을 따라야 합니다:



저작자표시. 귀하는 원저작자를 표시하여야 합니다.



비영리. 귀하는 이 저작물을 영리 목적으로 이용할 수 없습니다.



변경금지. 귀하는 이 저작물을 개작, 변형 또는 가공할 수 없습니다.

- 귀하는, 이 저작물의 재이용이나 배포의 경우, 이 저작물에 적용된 이용허락조건을 명확하게 나타내어야 합니다.
- 저작권자로부터 별도의 허가를 받으면 이러한 조건들은 적용되지 않습니다.

저작권법에 따른 이용자의 권리는 위의 내용에 의하여 영향을 받지 않습니다.

이것은 [이용허락규약\(Legal Code\)](#)을 이해하기 쉽게 요약한 것입니다.

[Disclaimer](#)

Master's Thesis

**Bioelectrochemical conversion of CO₂ to value
added product formate using engineered
*Methylobacterium extorquens***

Jungho Jang

Department of Chemical Engineering

Graduate School of UNIST

2018

**Bioelectrochemical conversion of CO₂ to value
added product formate using engineered
*Methylobacterium extorquens***

Jungho Jang

Department of Chemical Engineering

Graduate School of UNIST

**Bioelectrochemical conversion of CO₂ to value
added product formate using engineered
*Methylobacterium extorquens***

A thesis/dissertation
submitted to the Graduate School of UNIST
in partial fulfillment of the
requirements for the degree of
Master of Science

Jungho Jang

Month/Day/Year of submission

Approved by

Advisor

Yong Hwan Kim

**Bioelectrochemical conversion of CO₂ to value
added product formate using engineered
*Methylobacterium extorquens***

Jungho Jang

This certifies that the thesis/dissertation of Jungho Jang is approved.

06. 14. 2018

Advisor: Yong Hwan Kim

Sung Kuk Lee: Thesis Committee Member #1

Hyun-Kon Song: Thesis Committee Member #2

Abstract

Converting carbon dioxide to formate is a fundamental technology for building the C1 chemical platform. *Methylobacterium extorquens* AM1 (*M. extorquens* AM1) was reported to efficiently convert carbon dioxide to formate in an electrochemical carbon dioxide reduction system. In this study, formate dehydrogenase 1 of *M. extorquens* AM1 (MeFDH1) was verified as a key enzyme for the conversion of carbon dioxide to formate by testing MeFDH1 knock-out mutant. To increase expression level of MeFDH1, *M. extorquens* AM1 was engineered to harbor the recombinant expressing plasmid containing MeFDH1 gene tagged with hexahistidine. Recombinant *M. extorquens* AM1 cultured under optimal conditions showed a 2.5-fold higher formate productivity (2.53mM/g-wet cell/hr) than formate productivity of wild-type *M. extorquens* AM1. This result demonstrates that *M. extorquens* AM1 was successfully engineered to overexpress MeFDH1 and MeFDH1 is an essential enzyme for synthesis of formate from carbon dioxide. After optimizing the expression conditions of MeFDH1, the reaction conditions of the electrochemical reduction system were studied to improve the production efficiency of formate.

Contents

1. Introduction -----	1
2. Results and discussion -----	3
2.1. Determination of essential enzyme for formate production from CO ₂ in <i>M. extorquens</i> AM1 -----	3
2.2. Confirmation of recombinant MeFDH1 expressed from <i>M. extorquens</i> AM1 (F1A-P1) --	9
2.3. Optimized culture conditions for increasing MeFDH1 expression of mutant (F1A-P1) and formate production in an electrochemical CO ₂ reduction system -----	11
2.4. Optimization of electrochemical CO ₂ reduction system -----	18
3. Conclusion -----	24
4. Materials and methods -----	25
4.1. Microbial strain and culture condition-----	25
4.2. Gene-knockout system and one-step sequence-and ligation-independent cloning -----	26
4.3. Western blot analysis for MeFDH1 expression level-----	27
4.4. Electrochemical CO ₂ reduction system and formate analysis -----	28
4.5. MeFDH1 assays and purification-----	30
References-----	31

List of figures, table, and scheme

Figure 1. FPLC analysis of <i>M. extorquens</i> AM1 cell extract. -----	5
Figure 2. Protein identification result -----	6
Figure 3. Diagram of the gene-knockout system for the construction of <i>M. extorquens</i> AM1 mutants -----	7
Figure 4. Formate production of strains in the electrochemical reaction system -----	8
Figure 5. Time profile of MeFDH1 expression level-----	10
Figure 6. Relative expression level of MeFDH1 depending on methanol concentration -----	13
Figure 7. Relative expression level of MeFDH1 depending on cofactor(W) concentration-----	14
Figure 8. Western blotting of mutant (F1A-P1) crude extracts depending on cofactor(W) concentration -----	15
Figure 9. The relative formate production of the mutant (F1A-P1) with different type of electron mediators-----	16
Figure 10. The comparison between formate production of wild type and that of mutant (F1A-P1) cultured under optimum conditions-----	17
Figure 11. The formate productivity depending on type of working electrode-----	20
Figure 12. Faradaic efficiency depending on MeFDH1 unit-----	21
Figure 13. Faradaic efficiency depending on electron mediator concentration -----	22
Figure 14. Faradaic efficiency depending on reaction potential -----	23
Table 1. Bacterial strains and their plasmids for knockout or for recombinant expression -----	4
Scheme 1. Graphical abstract of electrochemical CO ₂ reduction system-----	29

Nomenclature

M. extorquens AM1: *Methylobacterium extorquens* AM1

MeFDH1: Formate dehydrogenase 1 from *Methylobacterium extorquens* AM1

FMN: Flavin Mononucleotide

MV: Methyl Viologen

EV: Ethyl Viologen

HPLC: High Performance Liquid Chromatography

FPLC: Fast Protein Liquid Chromatography

1. Introduction

The rapid development of a wide-range of industrial technologies using fossil fuel has led to drastically increased level of atmospheric carbon dioxide (CO₂).¹ Furthermore, a vast number of reports confirm that elevated carbon dioxide level in the atmosphere can be a determining factor of global warming via greenhouse effects.¹⁻³ The conversion of CO₂ to value-added chemicals has been posited as an indispensable technology to slow down the rate of atmospheric [CO₂] accumulation.⁴⁻⁵ Fortunately, CO₂ is a promising renewable source to produce environmentally friendly chemical platforms such as formate, dimethyl carbonate, its polymers and others.⁶

Among many candidates that could be produced from CO₂ as a feedstock, formate is reported as one of the most desirable bulk chemicals in terms of economic and environmental benefits.⁷ Especially, direct formate fuel cell (DFFC) converting formate to electrical energy is a solution for storing renewable energy because formate can easily store energy generated from various renewable sources such as wind, solar, and hydro. Additionally, formate can be safely transported compared with hydrogen gas because formate is non-flammable, non-toxic and moderately inert in environment.⁸⁻⁹

Despite promising potential, conventional conversion technologies for CO₂ into valuable compounds harbor critical limitations such as harsh reaction conditions and requirements of rare precious metal catalysts and expensive reducing agents such as hydride and hydrogen.¹⁰⁻¹¹ Even though electro-catalysis of carbon dioxide is a promising alternative given relative low costs of electrical energy, some chemical electro-catalysts frequently demonstrate insufficient reaction selectivity during the conversion of carbon dioxide to formate due to the production of significant ratio of hydrogen gas as by-product.¹² Accordingly, enzyme based electro-catalyzed production of formate from CO₂ has received greater attention due to exceptional selectivity to formate.¹³⁻¹⁷ However, effective oxygen tolerant biocatalysts capable of utilizing electrons supplied from cathode have been sought to render biocatalytic formate production from CO₂ feasible.¹⁸

Previously, our group reported a new approach for the conversion of CO₂ to formate through electro-catalysis using a whole-cell biocatalyst. *Methylobacterium extorquens* AM1 (*M. extorquens* AM1) as a whole-cell catalyst showed excellent formate production capability from CO₂ with high oxygen-stability in electrochemical reactors. However, the enzyme primarily responsible for the synthesis of formate from CO₂ remained unknown. Previous studies were focused on the optimization of reaction conditions such as electron mediators, cell mass concentration and pH value.¹⁹

In this study, we clearly demonstrate that formate dehydrogenase 1 (MeFDH1), a heterodimeric protein composed of alpha and beta subunits, is the essential enzyme in formate synthesis from CO₂ in *M. extorquens* AM1 cells. The MeFDH1 coding gene-knockout verified the role of this enzyme in the synthesis of formate from CO₂. In addition, we generated a homologous recombinant *M. extorquens*

AM1 expressing gene of MeFDH1 tagged with hexahistidine (6xHis-tag). Recombinant *M. extorquens* AM1 not only provide higher MeFDH1 expression than wild-type, but also allow us to confirm optically the expression level of MeFDH1 through Western blotting. Furthermore, the 6xHis-tag of recombinant MeFDH1 enables the easy and high purity purification using Ni-NTA resin. Various factors, including the concentration of metal ions (tungstate) and induction time using methanol as inducer, were optimized for improved MeFDH1 expression and increased formate conversion from CO₂ in MeFDH1 recombinant *M. extorquens* AM1. Also, we improved efficiency of electrochemical CO₂ reduction system using purified MeFDH1 by studying working electrode, reaction potential and the ratio of MeFDH1 to electron mediator.

2. Results and discussion

2.1. Determination of essential enzyme for formate production from CO₂ in *M. extorquens* AM1

The *M. extorquens* AM1 genome is known to contain four formate dehydrogenase coding genes (*fdh1*, *fdh2*, *fdh3* and *fdh4*).²⁰⁻²¹ Among these formate dehydrogenase coding genes, the *fdh1* gene for MeFDH1 (GenBank accession No. ACS42636.1(α-subunit), ACS42635.1(β-subunit)) was selected for the generation of *M. extorquens* AM1 knock-out mutants because MeFDH1 was assumed to be an essential enzyme for CO₂ reduction in our previous study using fast protein liquid chromatography (FPLC). Cell extract of *M. extorquens* AM1 was separated into several fractions using FPLC (Figure 1(a)). Some fractions showed CO₂ reduction activity in electrochemical reduction system. Protein sequence analysis with 34 and 35 fractions showing CO₂ reduction activity clearly suggested that MeFDH1 is responsible enzyme for the reduction of CO₂ to formate (Figure 2). Even though MeFDH1 was previously reported to be the principal formate dehydrogenase during whole-cell oxidation of supplied formate, there was no report for the CO₂ reducing activity of MeFDH1.²¹ Accordingly, three species of *M. extorquens* AM1 mutants summarized Table 1 were generated (Figure 3). As shown in Figure 4, while wild type (WT) and the MeFDH1 recombinant expression mutant (F1A-P1) could synthesize formate from CO₂ in the electrochemical reaction system, neither the MeFDH1 alpha knockout mutant (F1A) nor the MeFDH1 beta knockout mutant (F1AB-P1B) produced any detectible level of formate from CO₂. These results support the hypothesis that MeFDH1 is the key enzyme responsible for the conversion of CO₂ to formate. In addition, both the α- and β-subunits of MeFDH1 were proven simultaneously required for MeFDH1 to function properly. The α-subunit of MeFDH1 (MeFDH1α) is reported to contain binding sites for bis-tungstopterin guanine dinucleotide cofactor, three 4Fe4S clusters and one 2Fe2S cluster. The β-subunit of MeFDH1 (MeFDH1β) harbors binding sites for flavin mononucleotide (FMN), NAD⁺ and one 4Fe4S cluster.²² A purified recombinant β-subunit of MeFDH1 at atmosphere was successfully applied for the regeneration of NADH by utilizing methyl viologen as an artificial electron mediator in the electrochemical reactor.²³ This result implies that the β-subunit of MeFDH1 is essential for the reduction of CO₂ catalyzed by MeFDH1 since FMN of MeFDH1β may be the sole site to accept electrons from MV.

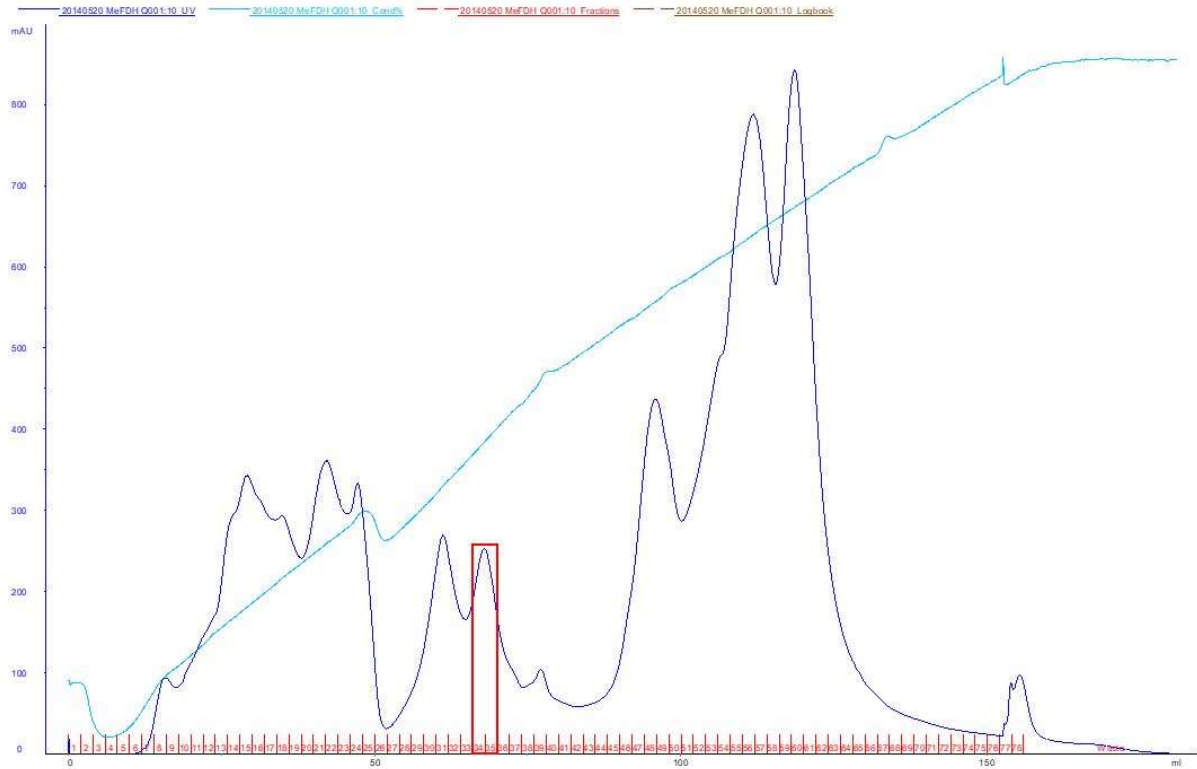
The *M. extorquens* AM1 mutant (F1A-P1) showed higher formate production (0.98 mM/hr/g-wet cell) compared to the formate production (0.68 mM/hr/g-wet cell) in WT *M. extorquens* AM1, as shown in Figure 4. The F1A-P1 strain harbored a homologously expressed recombinant MeFDH1 coded by pCM110(*fdh1*) since plasmid pCM110 contains *P_{mxoF}*, which was reported as a strong inducible promoter in *M. extorquens* AM1. This promoter can significantly increase the expression of MeFDH1

because of its high promoter strength compared to other promoters.²⁴ Based on results of Figure 4, we supposed that MeFDH1 expression *in vivo* can directly affect formate production.

Table 1. Bacterial strains and their plasmids for knockout or for recombinant expression.

Strain	Deletion gene	Knock-out plasmid	Recombinant plasmid	Selective antibiotic
Wild type	-	-	-	Rif
F1A	$\Delta fdh1\alpha$	pCM184($\Delta fdh1\alpha$)	-	Rif, Kan
F1A-P1	$\Delta fdh1\alpha$	pCM184($\Delta fdh1\alpha$) pCM157(<i>cre</i>)	pCM110(<i>fdh1</i>)	Rif, Tet
F1AB-P1B	$\Delta fdh1\alpha$ β	pCM184($\Delta fdh1\alpha$), pCM157(<i>cre</i>), pCM184($\Delta fdh1\beta$)	pCM110(<i>fdh1</i> α)	Rif, Kan, Tet

(a)



(b)

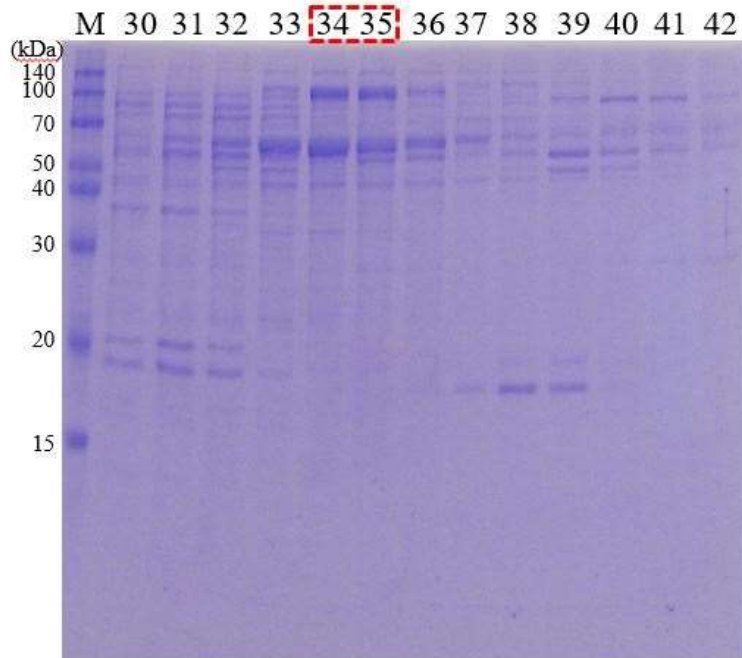


Figure 1. FPLC analysis of *M. extorquens* AM1 cell extract. (a) Fractions separated by two steps chromatographic (Hitrap SP HP and Hitrap Q HP, GE healthcare Life Science), (b) SDS-PAGE of fractions: protein marker (M), fraction numbers (30~42).


Mascot Search Results

gi|489699156 Mass: 107273 Score: 809 Matches: 30(6) Sequences: 16(5) emPAI: 0.20

formate dehydrogenase subunit alpha [Methylobacterium extorquens]

Check to include this hit in error tolerant search

Query	Observed	Mr (expt)	Mr (calc)	Delta	Miss	Score	Expect	Rank	Unique	Peptide
169	597.5551	1193.0957	1192.5216	0.5741	0	44	8.7	2		R.ACMVRIEGER.V + Carbamidomethyl (C)
<input checked="" type="checkbox"/> 173	610.3266	1218.6387	1218.5517	0.0871	0	61	0.18	1		R.EATWEEALDR.A
174	611.1366	1220.2587	1218.5517	1.7071	0	(33)	1.1e+02	4		R.EATWEEALDR.A
182	643.3021	1284.5897	1284.5986	-0.0089	0	79	0.0031	2		K.GSNEEAYLQK.L
<input checked="" type="checkbox"/> 202	711.7576	1421.5007	1421.6643	-0.1636	0	(56)	0.6	1		K.MASVCGIDAETLR.E + Carbamidomethyl (C)
<input checked="" type="checkbox"/> 205	719.7436	1437.4727	1437.6592	-0.1865	0	67	0.043	1		K.MASVCGIDAETLR.E + Carbamidomethyl (C); Oxidation (M)
<input checked="" type="checkbox"/> 214	746.2621	1490.5097	1490.7001	-0.1904	0	35	78	1	U	K.SGQQAAPDFSGSYGIK.D
<input checked="" type="checkbox"/> 215	747.7366	1493.4587	1492.7344	0.7243	0	(64)	0.093	1		R.EVQVNDVIGMAYR.A
<input checked="" type="checkbox"/> 218	755.3856	1508.7567	1508.7293	0.0274	0	87	0.00047	1		R.EVQVNDVIGMAYR.A + Oxidation (M)
<input checked="" type="checkbox"/> 219	756.1901	1510.3657	1508.7293	1.6364	0	(73)	0.0098	1		R.EVQVNDVIGMAYR.A + Oxidation (M)
222	759.3176	1516.6207	1516.8362	-0.2155	0	(39)	32	2	U	R.VQIAQPVVAPPGDAR.Q
<input checked="" type="checkbox"/> 223	760.5751	1519.1357	1517.8202	1.3155	0	41	20	1	U	R.VQIAQPVVAPPGDAR.Q + Deamidated (NQ)
<input checked="" type="checkbox"/> 235	801.7876	1601.5607	1600.7957	0.7650	0	76	0.0053	1	U	R.IVYAEQVNGPANQR.L
247	837.4481	1672.8817	1672.9373	-0.0556	1	29	3e+02	6	U	R.RVQIAQPVVAPPGDAR.Q
<input checked="" type="checkbox"/> 283	889.7201	1777.4257	1776.7634	0.6624	0	56	0.54	1	U	K.SLCPYCGVCGQVSYK.V + 3 Carbamidomethyl (C)
<input checked="" type="checkbox"/> 289	914.9961	1827.9777	1827.9440	0.0337	0	(60)	0.23	1		R.AGVLDALPEAVAFMAFK.E
<input checked="" type="checkbox"/> 304	923.2381	1844.4617	1843.9390	0.5228	0	69	0.029	1		R.AGVLDALPEAVAFMAFK.E + Oxidation (M)
<input checked="" type="checkbox"/> 313	941.4621	1880.9097	1881.8394	-0.9297	0	33	1e+02	1		K.DANDQVDPANFWTFR.E
<input checked="" type="checkbox"/> 351	993.2311	1984.4477	1984.0452	0.4026	1	(30)	2.4e+02	1		R.RAGVLDALPEAVAFMAFK.E
<input checked="" type="checkbox"/> 354	1001.0071	1999.9997	2000.0401	-0.0403	1	(42)	15	1		R.RAGVLDALPEAVAFMAFK.E + Oxidation (M)
<input checked="" type="checkbox"/> 355	1001.9636	2001.9127	2000.0401	1.8727	1	59	0.29	1		R.RAGVLDALPEAVAFMAFK.E + Oxidation (M)
393	729.8219	2186.4437	2185.9521	0.4917	0	(37)	44	3		R.GMPFVEGENPAMSDPDLNHAR.H
394	1094.3426	2186.6707	2186.9361	-0.2654	0	(24)	9.2e+02	2		R.GMPFVEGENPAMSDPDLNHAR.H + Deamidated (NQ)
<input checked="" type="checkbox"/> 397	1102.0271	2202.0397	2201.9470	0.0927	0	59	0.27	1		R.GMPFVEGENPAMSDPDLNHAR.H + Oxidation (M)
<input checked="" type="checkbox"/> 398	735.1815	2202.5227	2202.9310	-0.4083	0	(51)	1.7	1		R.GMPFVEGENPAMSDPDLNHAR.H + Oxidation (M); Deamidated (NQ)
400	1110.1761	2218.3377	2217.9419	0.3958	0	(30)	2.1e+02	4		R.GMPFVEGENPAMSDPDLNHAR.H + 2 Oxidation (M)
<input checked="" type="checkbox"/> 401	740.5075	2218.5007	2218.9259	-0.4252	0	(48)	3.7	1		R.GMPFVEGENPAMSDPDLNHAR.H + 2 Oxidation (M); Deamidated (NQ)
<input checked="" type="checkbox"/> 468	1333.1791	2664.3437	2663.3517	0.9921	0	25	6.2e+02	1	U	K.IVPAIVPEDEVPDEFPMVLTGR.V
<input checked="" type="checkbox"/> 471	894.2612	2679.7617	2679.3466	0.4151	0	(25)	6.9e+02	6	U	K.IVPAIVPEDEVPDEFPMVLTGR.V + Oxidation (M)
533	1599.7131	3197.4117	3197.4829	-0.0712	0	51	1.6	2	U	R.EGAVTYFVDAPDQGNRIIFYAGFPFTESGR.A + Deamidated (NQ)

Figure 2. Protein identification result by protein search engine (Mascot, Matrix Science). *M. extorquens* AM1 alpha subunit showed the highest score.

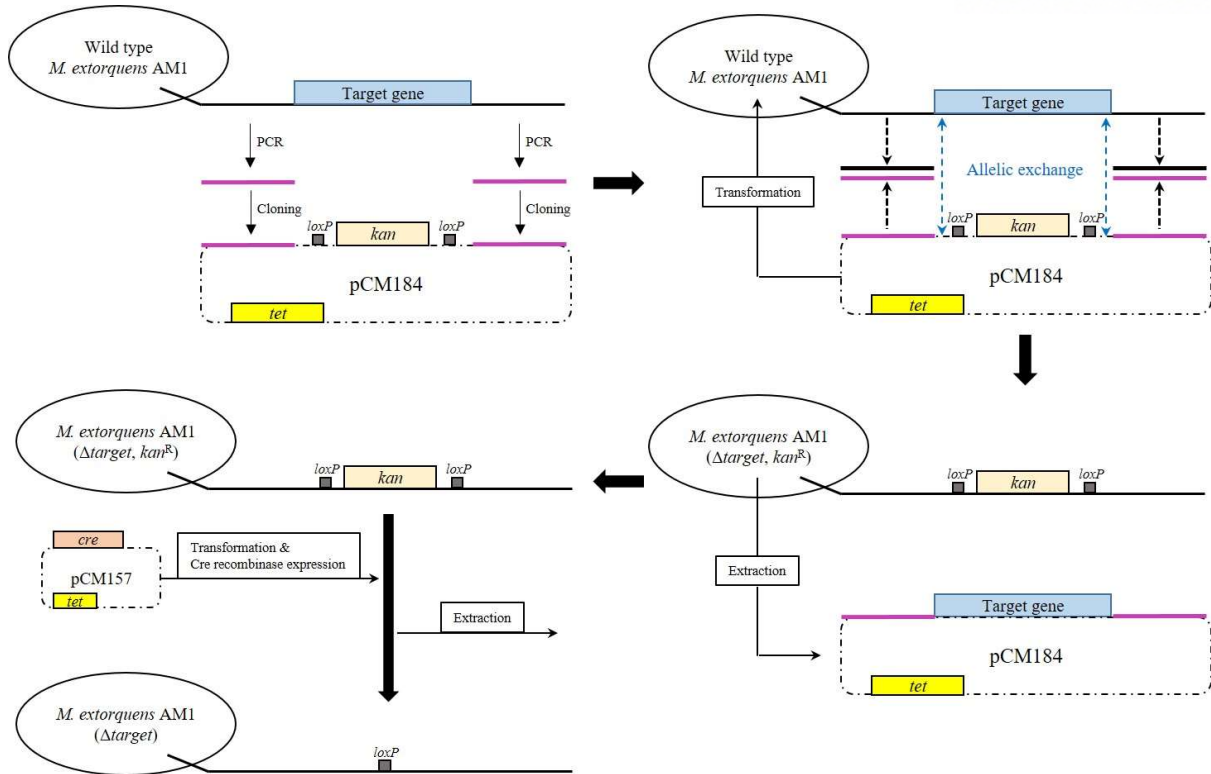


Figure 3. Diagram of the gene-knockout system for the construction of *M. extorquens* AM1 mutants. Sequences located on both sides of the target gene in the genome of *M. extorquens* AM1 were amplified by PCR and cloned into pCM184. The target gene was exchanged with the *loxP-kan-loxP* gene through homologous allelic recombination between *M. extorquens* AM1 and pCM184. For extraction of pCM184, *M. extorquens* AM1 mutants (Δ target, *Kan*^R) were cultivated in media without kanamycin. Next, *cre* recombinase was expressed on pCM157 to eliminate the kanamycin resistance gene between *loxP* genes through site-specific recombination.

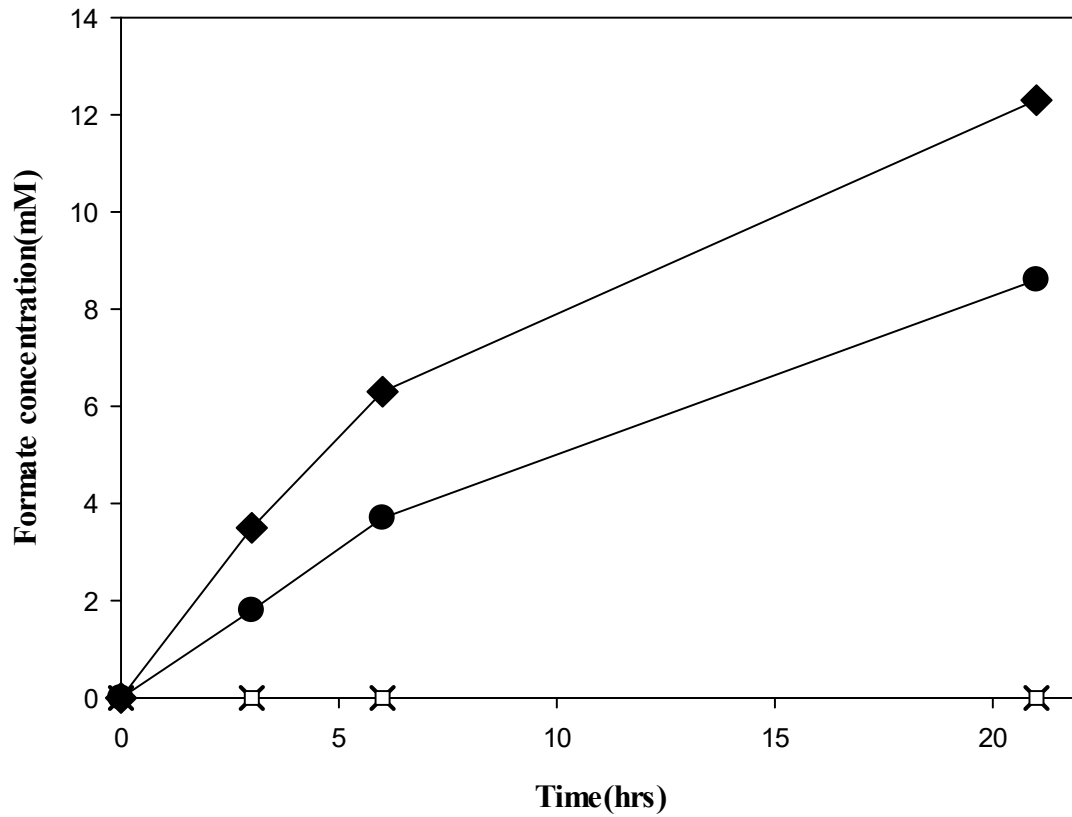
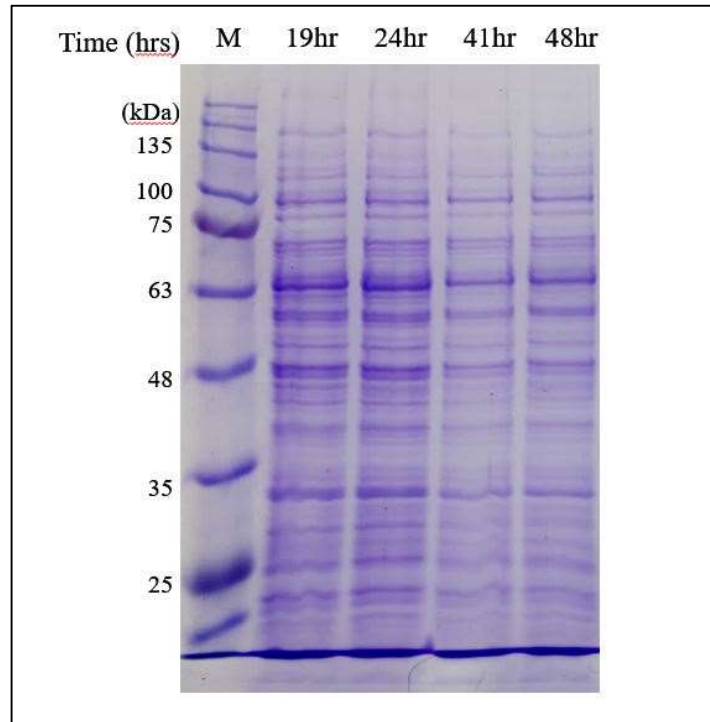


Figure 4. Formate production of strains in the electrochemical reaction system: F1A-P1 (◆), WT (●), F1A (X), F1AB-P1B (□), reaction conditions: 0.6 g wet-cell, 10 mM MV, pH 6.0, -0.75V (vs AgCl); CO₂ gas purging (99.999%, rate: 1 mL/s).

2.2. Confirmation of recombinant MeFDH1 expressed from *M. extorquens* AM1 (F1A-P1)

The crude lysate of homologously expressed recombinant (F1A-P1) was used for SDS-PAGE and Western blotting to analyze the expression level of MeFDH1 in *M. extorquens* AM1 (F1A-P1). The target bands for MeFDH1 α and MeFDH1 β were difficult to distinguish due to their relatively weak expression in SDS-PAGE (see Figure 5(a)) despite molecular weight estimates of 108 kDa and 62 kDa, respectively. However, the α -subunit and β -subunit of MeFDH1 were clearly confirmed through western blotting as shown in Figure 5(b). Interestingly, expression of MeFDH1 α appeared slightly decreased after the 41 hours incubation, even though the recovered expression level was observed repeatedly at 48 hours. These observations imply that a considerable fraction of homologously expressed recombinant MeFDH1 can be degraded through endogenous metabolism.²⁵

(a)



(b)

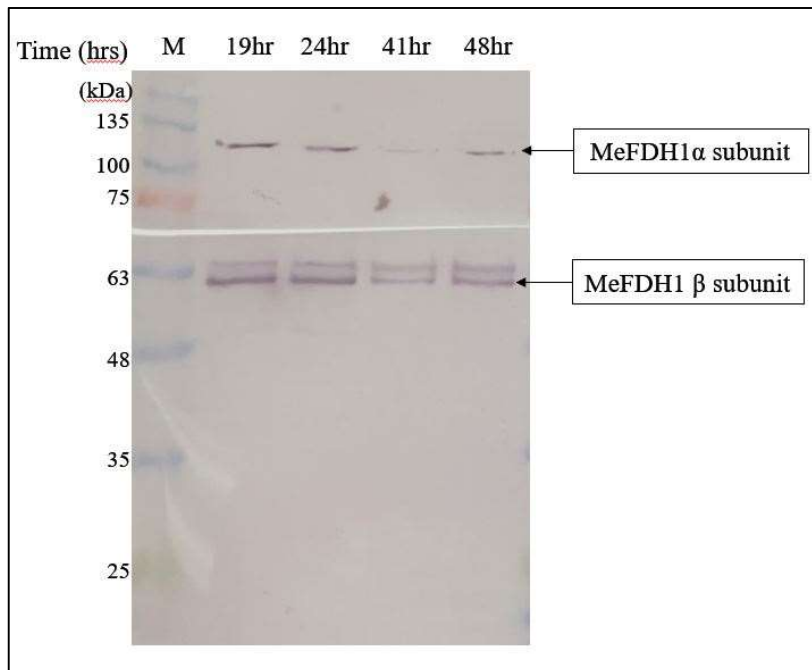


Figure 5. Time profile of MeFDH1 expression level. (a) SDS-PAGE (10%) of mutant (F1A-P1) crude extracts, (b) Western blotting of mutant (F1A-P1) crude extracts: protein marker (M), incubation times (19hr, 24hr, 41hr, 48hr).

2.3. Optimized culture conditions for increasing MeFDH1 expression of mutant (F1A-P1) and formate production in an electrochemical CO₂ reduction system

Methanol was added to the culture medium to induce the expression of MeFDH1, as well as to supply a carbon source for *M. extorquens* AM1 since expression of MeFDH1 is controlled by the methanol-inducible promoter P_{mxaf} .²⁴ The methanol concentration in the culture medium affected MeFDH1 expression in mutant (F1A-P1). Figure 6 shows that the higher methanol concentration produces greater MeFDH1 expression in mutant (F1A-P1), especially after a 48 hours incubation. As predicted, mutant (F1A-P1) cultured in medium with initial 2.0% methanol concentration showed 2.11 mM-formate/hr/g-wet cell as the highest formate production rate in the electrochemical CO₂ reduction system. This result strongly supports our hypothesis that MeFDH1 expression has a proportional relationship with the formate production through CO₂ reduction. In other words, much higher expression of MeFDH1 is expected to result in the higher production of formate since recombinant MeFDH1 is the critical limiting biocatalyst.

Unlike other common formate dehydrogenases, MeFDH1 is known to contain W-pterin guanidine dinucleotide instead of Mo as its prosthetic group.²¹ Generally, the availability of tungsten is reported to be much lower compared to its counterpart molybdenum.²⁶ Even though chemical properties of W and Mo are known to be quite similar, microbes appear to prefer one over the other based on its specific transporter.²⁷ Tungstate concentration initially added in the culture medium also affected the MeFDH1 expression level of mutant (F1A-P1). As shown in Figure 7, mutant (F1A-P1) cultured in 2x tungstate (60 μM) resulted in increased expression of MeFDH1. However, 4x tungstate (120 μM) did not increase the expression of MeFDH1. This result may be related to observations that high concentrations of tungstate and W-pterin guanidine dinucleotide cofactor intermediates in the pterin pathway can cause cellular toxicity.²⁸⁻²⁹ Interestingly, optimum concentration of tungstate seems to repress the degradation of recombinant MeFDH1 (Figure 8), which implies that tungstate deficiency may cause improper production of apoprotein, and apoprotein may be more vulnerable to endogenous degradation.³⁰

An artificial electron mediator was used for the electron transfer from copper plate cathode to MeFDH1 in electrochemical CO₂ reduction system. Among many electron mediators, the mutant (F1A-P1) produced formate from CO₂ when methyl viologen (MV) and ethyl viologen (EV) were employed as electron mediator, on the while other mediator such as FMN and NR did not work with the mutant (F1A-P1). (Figure 9). Additionally, there are other papers reporting that MV was most suitable electron mediator for CO₂ reduction reaction in electrochemical system using tungsten containing formate dehydrogenase.³¹⁻³²

Based on the experimental results shown in Figure 6 and 7, the balance between the expression level of the apo-form and the flux rate of its cofactor pathway may be an indispensable requirement to

obtain a significant quantity of the holo-form of MeFDH1 in *M. extorquens* AM1. The mutant (F1A-P1) produced over 30 mM of formate from carbon dioxide within 24 hours in electrochemical reactions. This was three times greater than the production of wild type *M. extorquens* AM1 at optimal methanol and tungstate concentrations (Figure 10). Wild-type *M. extorquens* AM1, however, showed 0.77 mM/hr/g-wet cell, which is three times lower than that of recombinant mutant (F1A-P1). Furthermore, a less significant difference between optimum conditions and previous conditions was observed (Figure 10). This result demonstrates that in contrast with the promoter P_{mxaF} of recombinant mutant (F1A-P1), the unknown promoter of the gene encoding MeFDH1 of *M. extorquens* AM1 wild type was not affected by methanol or tungstate concentrations in culture medium. Until now, the production of formate from carbon dioxide was proportional to the level of expression in recombinant MeFDH1. Consequently, a strong and simply regulated promoter such as P_{mxaF} was a core factor for homologous expression of recombinant MeFDH1 with an optimal tungstate concentration in the medium.

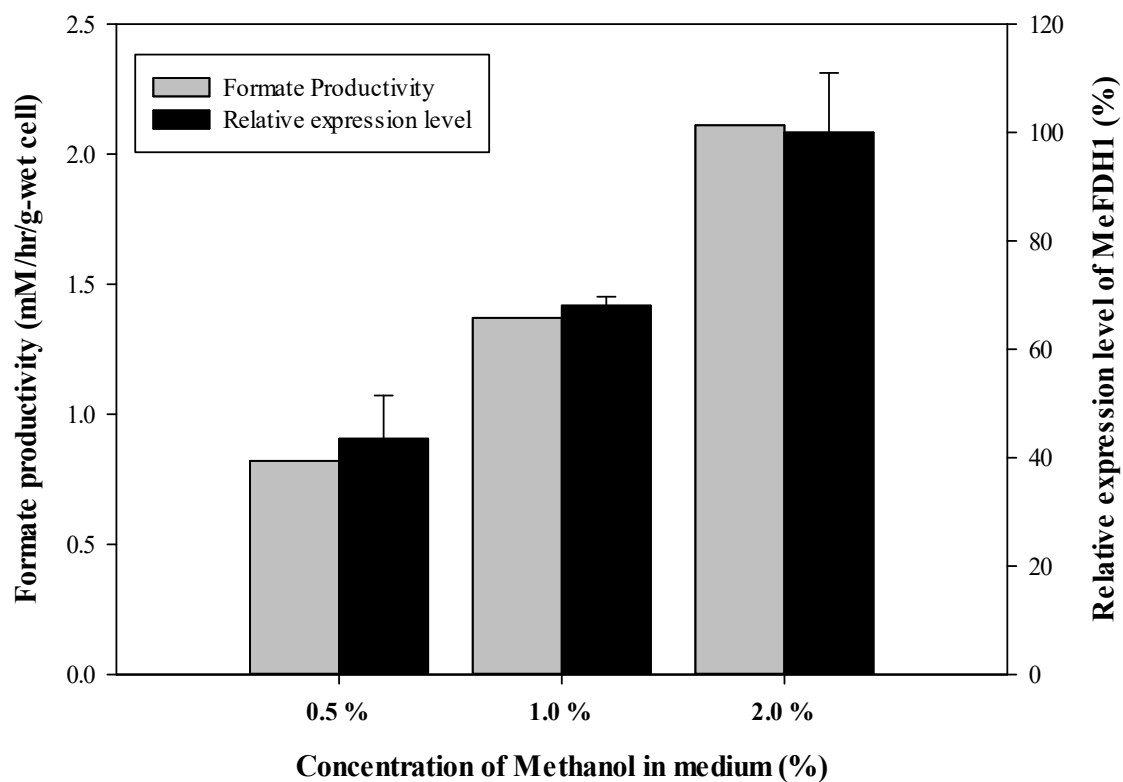


Figure 6. Relative expression level of MeFDH1 depending on methanol concentration and formate productivity in electrochemical CO₂ reduction system (0.6 g wet-cell, 10 mM MV, pH 6.0, -0.75V (vs AgCl); CO₂ gas purging (99.999%, rate: 1 mL/s)).

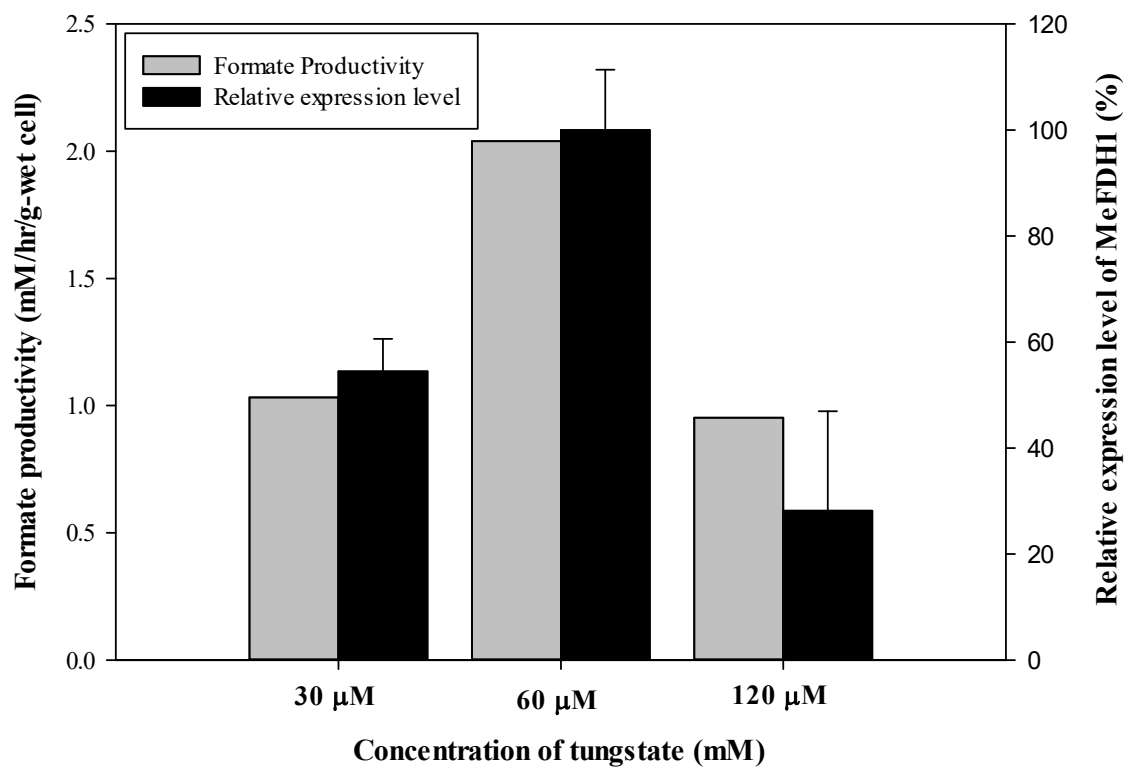


Figure 7. Relative expression level of MeFDH1 depending on cofactor(W) concentration and formate productivity in electrochemical CO₂ reduction system (0.6 g wet-cell, 10 mM MV, pH 6.0, -0.75V (vs AgCl); CO₂ gas purging (99.999%, rate: 1 mL/s)).

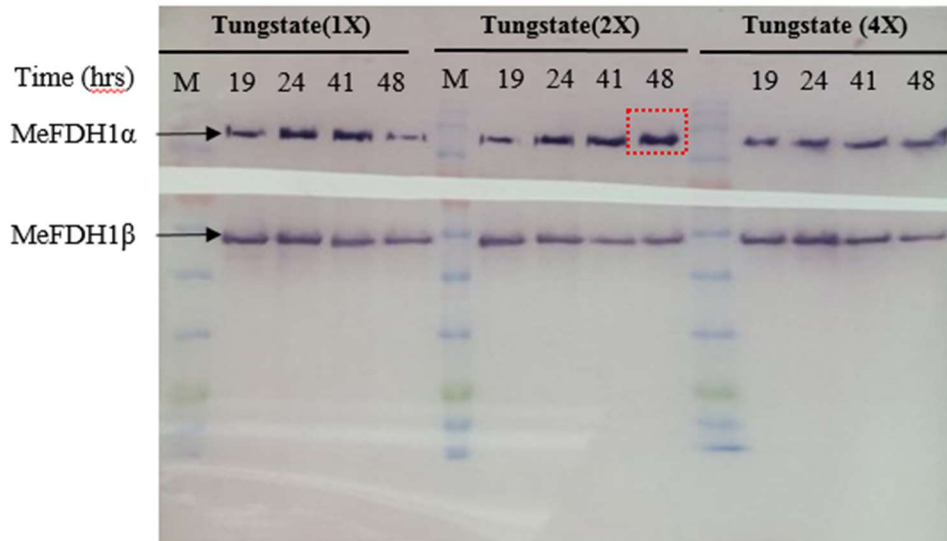


Figure 8. Western blotting of mutant (F1A-P1) crude extracts depending on cofactor(W) concentration: 1x tungstate (30 μ M), 2x tungstate (60 μ M), 4x tungstate (120 μ M), protein marker (M), and incubation times (19hr, 24hr, 41hr, 48hr).

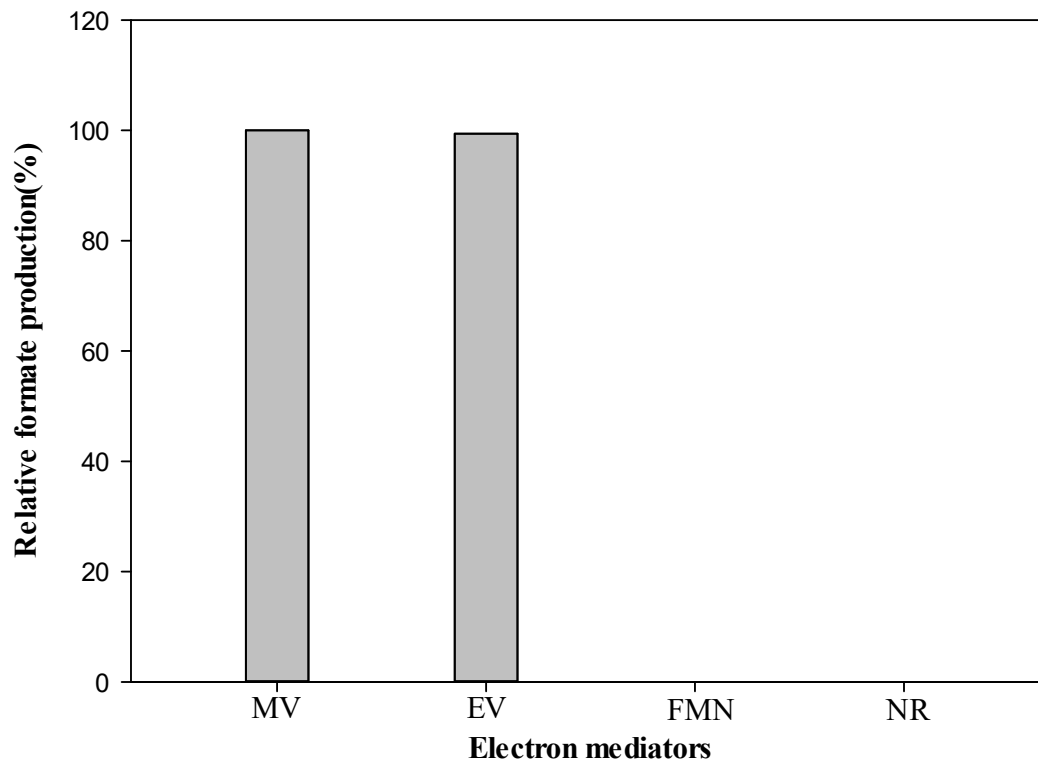


Figure 9. The relative formate production of the mutant (F1A-P1) with different type of electron mediators in electrochemical CO₂ reduction system: methyl viologen (MV), ethyl viologen (EV), flavin mononucleotide (FMN) and neural red (NR).

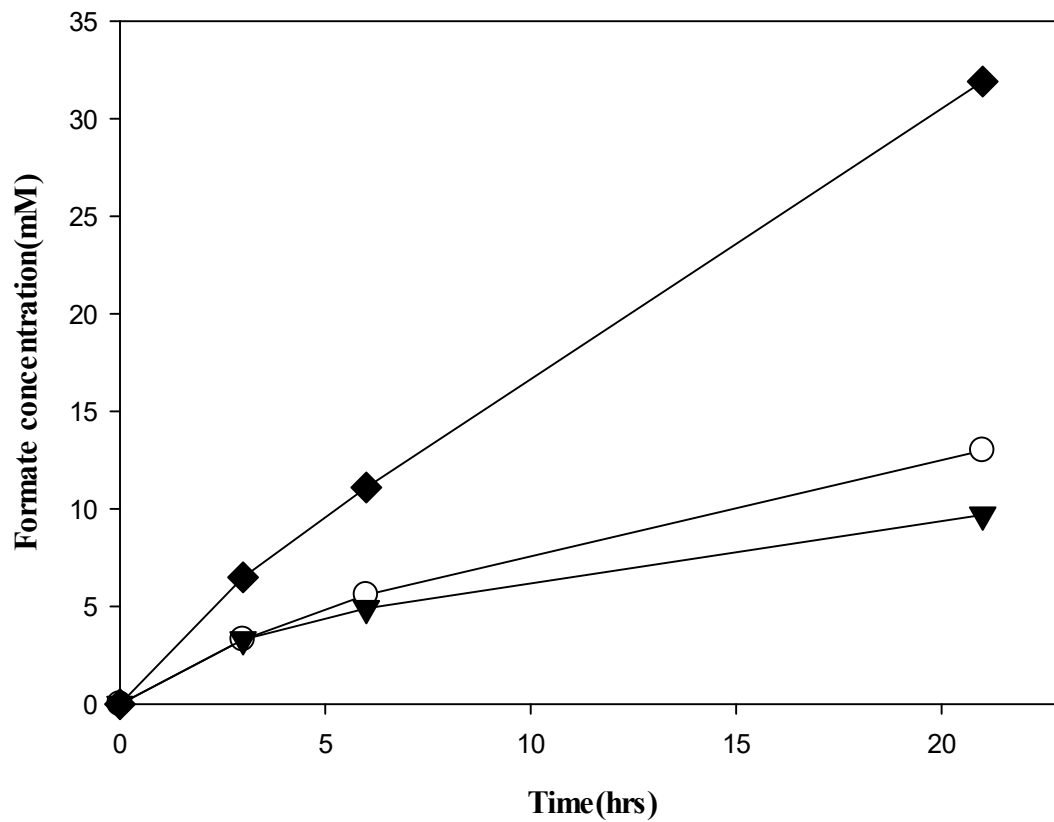


Figure 10. The comparison between formate production of wild type and that of mutant (F1A-P1) cultured under optimum conditions: WT cultured in basic conditions (0.5% (v/v) MeOH, 1x tungstate(30 μ M)) (○), WT cultured in optimum conditions (2.0% (v/v) MeOH, 2x tungstate(60 μ M)) (▼), F1A-P1 cultured in optimum conditions (2.0% (v/v) MeOH, 2x tungstate(60 μ M)) (0.6 g wet-cell, 10 mM MV, pH 6.0, -0.75V (vs AgCl); CO₂ gas purging (99.999%, rate: 1 mL/s)) (◆).

2.4. Optimization of electrochemical CO₂ reduction system

The working electrode reduces the electron mediator and provides an environment in which the MeFDH1 can synthesize formate from CO₂. However, the copper ions produced by copper plate as working electrode decrease the activity of MeFDH1.³³⁻³⁴ To avoid toxicity of copper ions, several types of electrodes were compared. As shown in Figure 11, all candidates showed higher formate productivity than copper plate. Among them, carbon felt showed the highest formate productivity because the largest surface area. In addition, since carbon felt is cheaper than other electrodes, it is advantageous for scale-up. Based on these results, the copper plate electrode was replaced with a carbon felt.

After confirming that MeFDH1 is an essential enzyme for CO₂ reduction, we confirmed the faradaic efficiency of electrochemical CO₂ reduction system depending on the ratio of MeFDH1 unit (U) to electron mediator. One unit (U) means the conversion of 1 micro-mole of substrate per minute. Figure 12 showed faradaic efficiency depending on MeFDH1 unit (U). There was no difference in the faradaic efficiency depending on the MeFDH1 unit. Therefore, the unit (U) of MeFDH1 was fixed at 25 and the faradaic efficiency depending on the concentration of electron mediator was measured. As shown in Figure 13, when the CO₂ reduction reaction was conducted using 10mM EV, the faradaic efficiency was about 70%. In other conditions (0.1mM, 1mM, and 5mM of EV), the faradaic efficiency was about 80%. The reason for decrease in efficiency is the dimerization of viologen. The irreversible radical cation dimerization of viologen consumed electrons and decreased the efficiency of formate production. The higher concentration of viologen, the easier irreversible dimerization occurs. Therefore, the lowest faradaic efficiency was obtained when using 10mM EV. The dimerization of viologen has been reported in several articles.³⁵⁻³⁶

The reaction potential affects faradaic efficiency. Figure 14 showed faradaic efficiency depending on potential. When the reaction potential was -0.54V or -0.94V (vs AgCl), formate was not detected by high-performance liquid chromatography (HPLC) analysis. Since the average current was less than 50 micro-amperes at -0.54V (vs AgCl), the concentration of formate was too low to perform the HPLC analysis even if the formate was synthesized by MeFDH1. On the other hand, at -0.94V (vs AgCl) relatively high current initially flowed, but the electron transport ability of EV was lost during the stabilization process due to dimerization of viologen, so that the formate was not synthesized. In other potential conditions, the efficiency was more than 80%. However, this value was calculated without considering the base current when the MeFDH1 is not added. Considering the base current, faradaic efficiency is over 99%. The reason for this high result is that the base current value under the MeFDH1 added condition is lower than the predicted current. If the amount of hydrogen gas produced during reaction can be measured, a more accurate faradaic efficiency can be obtained.

From these results we can confirm faradaic efficiency of electrochemical CO₂ reduction system

depending on various conditions such as enzyme unit, electron mediator concentration and reaction potential. In particular, we demonstrated that MeFDH1 efficiently convert CO_2 to formate at -0.64V (vs AgCl), which is the thermodynamic reduction potential of CO_2 in aqueous solution. However, in terms of productivity, the formate productivity of -0.64V (vs AgCl) condition was 5 times lower than the condition of -0.84V (vs AgCl). This result was derived from the difference in the reduction rate of EV. Therefore, if the concentration of EV or the surface area of the electrode were increased, high formate productivity can be expected at -0.64V (vs AgCl).

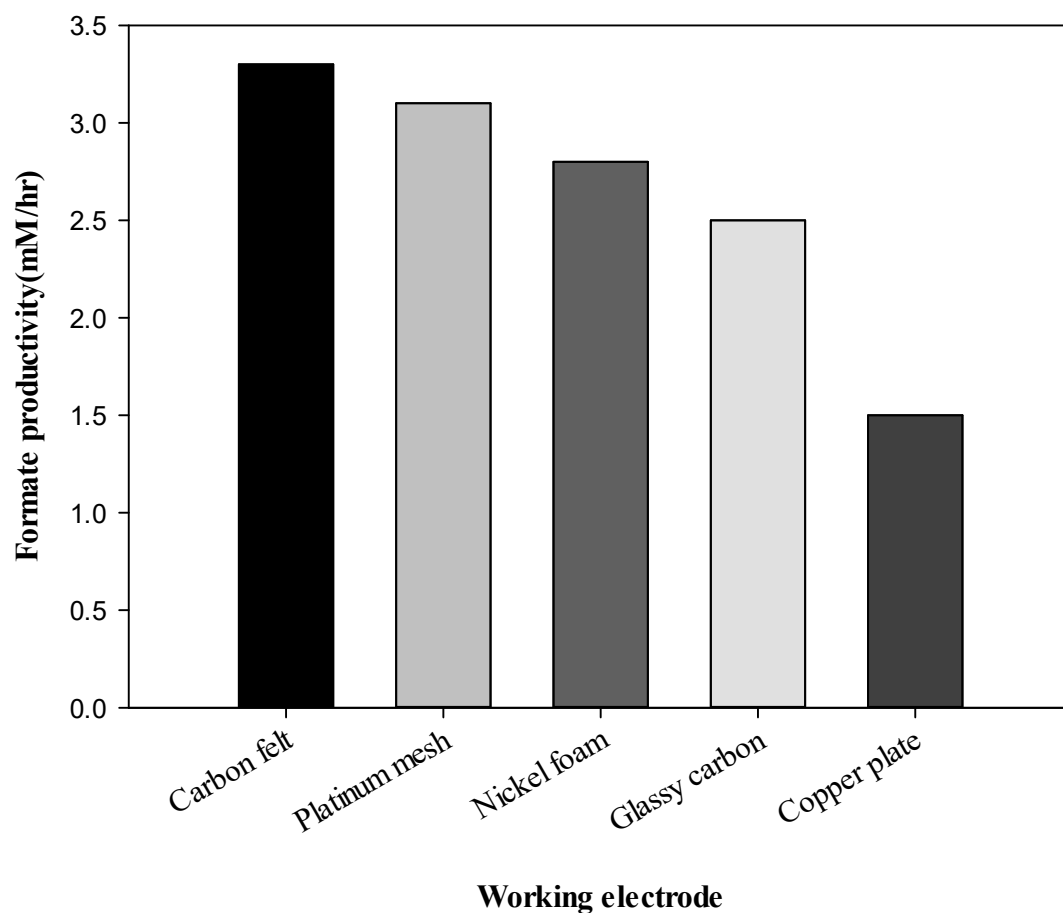


Figure 11. The formate productivity depending on type of working electrode in electrochemical CO₂ reduction system (1 mg MeFDH1, 10 mM MV, pH 7.0, -0.75V (vs AgCl); CO₂ gas purging (99.999%, rate: 1 mL/s)).

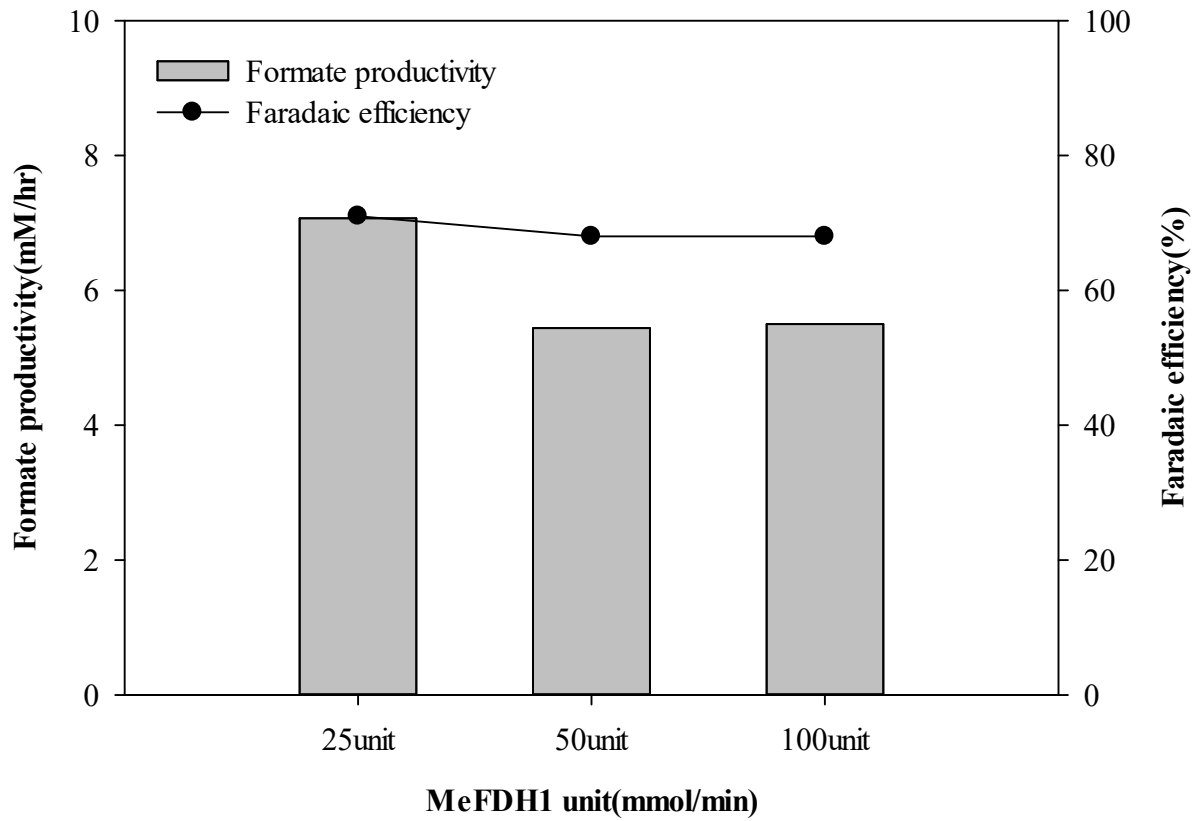


Figure 12. Faradaic efficiency depending on MeFDH1 unit (25-100unit MeFDH1, 10mM EV, pH 7.0, -0.75V (vs AgCl); CO₂ gas purging (99.999%, rate: 1 mL/s))

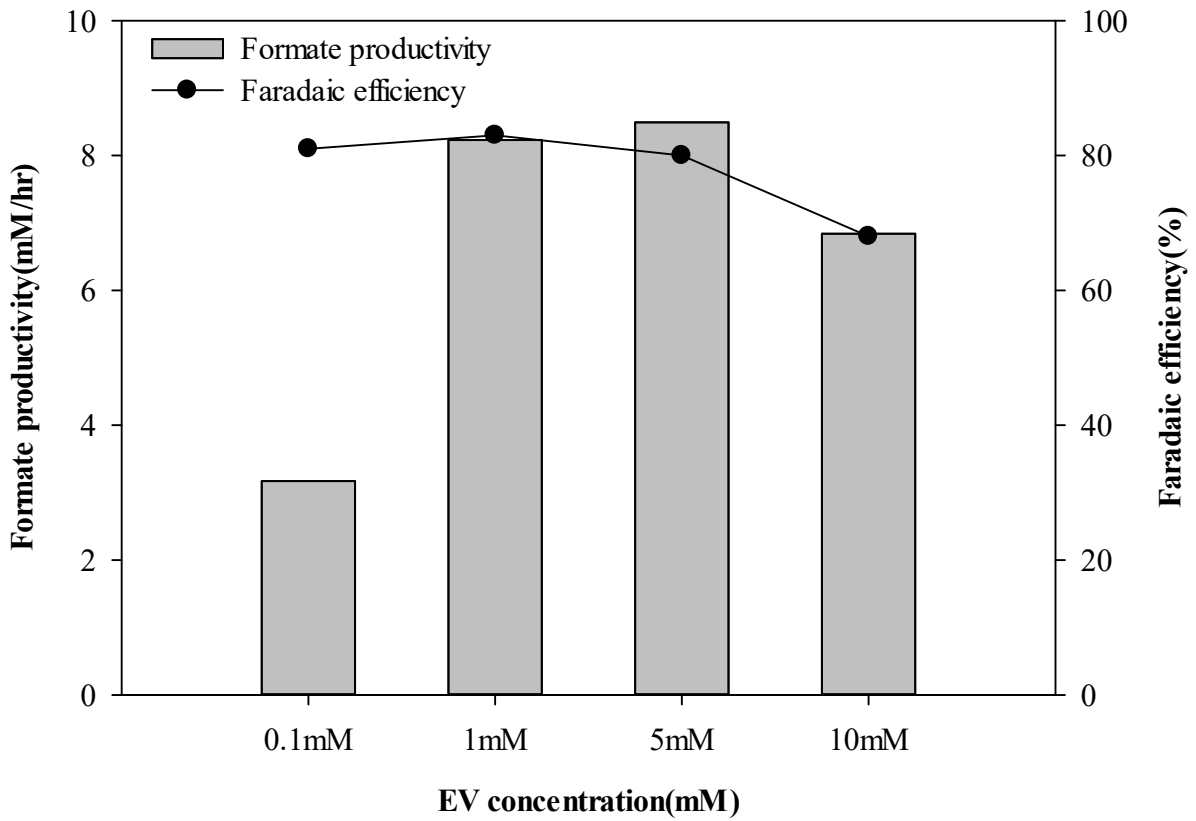


Figure 13. Faradaic efficiency depending on electron mediator concentration (25unit MeFDH1, 0.1-10mM EV, pH 7.0, -0.75V (vs AgCl); CO₂ gas purging (99.999%, rate: 1 mL/s))

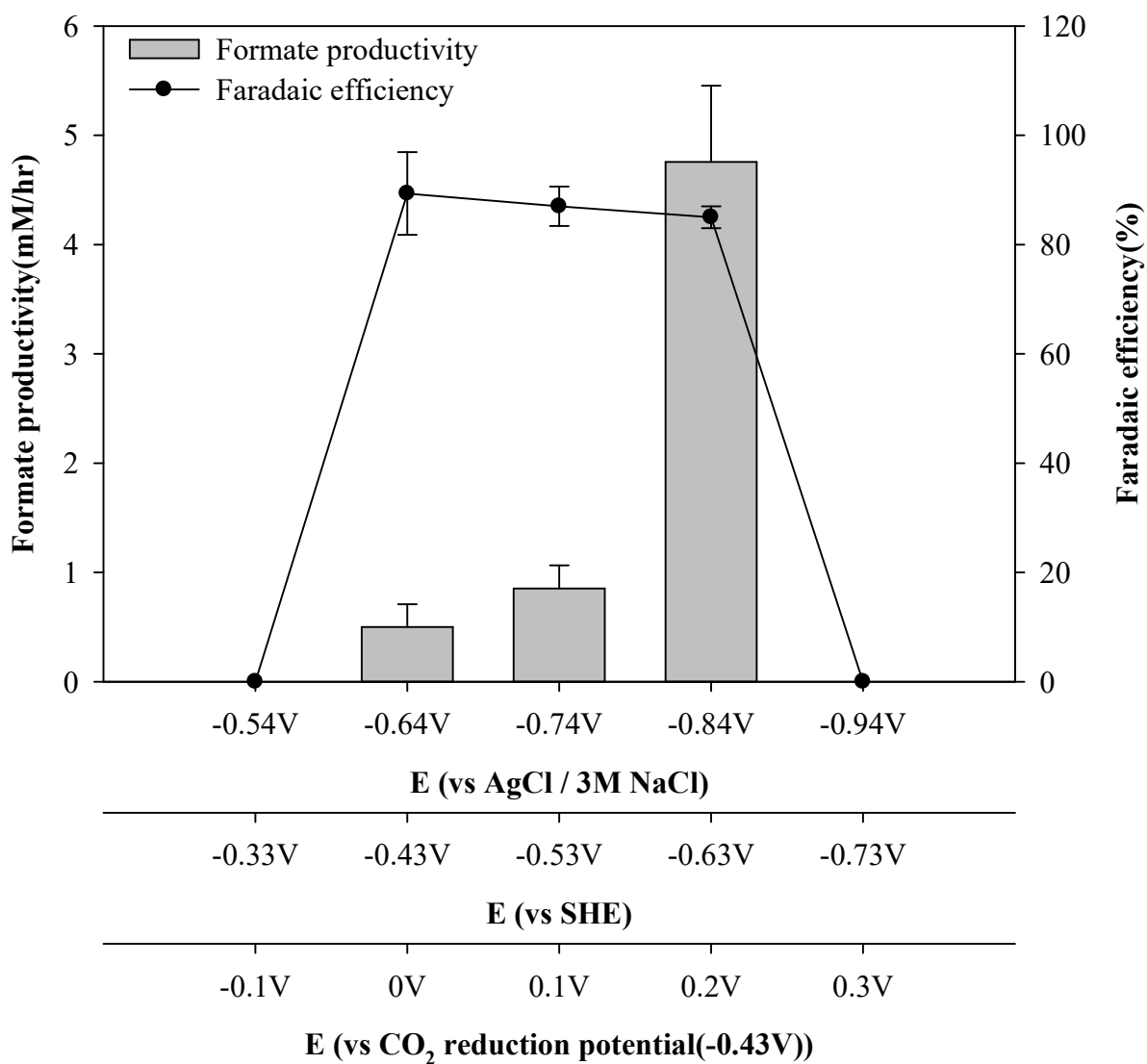


Figure 14. Faradaic efficiency depending on reaction potential (25unit MeFDH1, 0.1mM EV, pH 7.0, -0.54V~-0.94V (vs AgCl); CO₂ gas purging (99.999%, rate: 1 mL/s))

3. Conclusion

The genetic engineering of *M. extorquens* AM1 and optimization of culture conditions allowed improved formate production in electro-biocatalysis. Importantly, this study demonstrated that MeFDH1 is a critical enzyme in the catalysis of carbon dioxide to produce formate. Furthermore, the expression level of recombinant MeFDH1 and the tungstate concentration as a MeFDH1 cofactor significantly improved microbial formate production. Engineered *M. extorquens* AM1 demonstrated enhanced production of formate, reaching 2.53 mM/hr/g-wet cell, 2.5 times greater than wild type *M. extorquens* AM1. These results clearly showed the microbe genetic engineering is able to enhance whole-cell biocatalyst activity. In addition, the optimization of electrochemical CO₂ reduction system demonstrated faradaic efficiency of over 85% at low voltages. Based on the conditions of 85% efficiency, -0.74V (vs AgCl) and 90KRW per kWh, the production cost of 1 ton of formate is about 200USD which is 3times lower than conventional production cost (about 602USD). Although the calculation considers only electricity charges, this result suggests that electrochemical CO₂ reduction system using MeFDH1 can play an important role in reducing CO₂ emissions economically.

4. Materials and methods

4.1. Microbial strain and culture condition

Methylobacterium extorquens AM1 (ATCC 14781, GenBank accession No. CP001510.1) was used in this study. Culture medium was composed of a carbon source (16 g/L succinate) and minimal salt medium supplemented with trace elements and sodium tungstate. Minimal salt medium contained 1.62 g/L NH_4Cl , 0.2 g/L MgSO_4 , 2.21 g/L K_2HPO_4 , and 1.25 g/L $\text{NaH}_2\text{PO}_4 \cdot 2\text{H}_2\text{O}$. Trace elements contained 15 mg/L $\text{Na}_2\text{EDTA}_2 \cdot \text{H}_2\text{O}$, 4.5 mg/L $\text{ZnSO}_4 \cdot 7\text{H}_2\text{O}$, 0.3 mg/L $\text{CoCl}_2 \cdot 6\text{H}_2\text{O}$, 1 mg/L $\text{MnCl}_2 \cdot 4\text{H}_2\text{O}$, 1 mg/L H_3BO_3 , 2.5 mg/L CaCl_2 , 0.4 mg/L of $\text{Na}_2\text{MoO}_4 \cdot 2\text{H}_2\text{O}$, 3 mg/L $\text{FeSO}_4 \cdot 7\text{H}_2\text{O}$, and 0.3 mg/L $\text{CuSO}_4 \cdot 5\text{H}_2\text{O}$. After incubation for 19 hours, methanol (final concentration: 124 mM) was added as an inducer. The final concentration of antibiotics was 50 $\mu\text{g}/\text{mL}$ rifamycin (Rif), 50 $\mu\text{g}/\text{mL}$ kanamycin (Kan) and 10 $\mu\text{g}/\text{mL}$ tetracycline (Tet) in culture medium. Incubation proceeded at 26°C in 1 L Erlenmeyer shake flasks (200 mL working volume) in a 200-rpm shaking incubator.

4.2. Gene-knockout system and one-step sequence-and ligation-independent cloning (SLIC)

Gene-knockout was performed as described previously.³⁷ DNA located both upstream and downstream of tMeFDH1 (GenBank accession No. ACS42636.1(α -subunit), ACS42635.1(β -subunit)) was amplified by PCR. These sequences were cloned to locate both sides of the *loxP* and kanamycin genes of pCM184 (Addgene plasmid 46012). When *M. extorquens* AM1 was transformed with pCM184, allelic exchange occurred and *M. extorquens* AM1 acquired *loxP* and kanamycin genes but lost a partial gene sequence of MeFDH1. When *M. extorquens* AM1 was transformed with pCM157 (Addgene plasmid 45863), *cre* recombinase expressed on pCM157 extracted the kanamycin gene between the *loxP* sites through site-specific recombination. When *M. extorquens* AM1 was transformed with pCM110 containing MeFDH1 gene, MeFDH1 expression of *M. extorquens* AM1 was recovered. For all cloning, one-step SLIC was applied.³⁸ SLIC uses T4 DNA polymerase as exonuclease. This vector was linearized by restriction enzymes and sequences generated by PCR. NEB 2.1 buffer (B7202S, BioLabs) and T4 polymerase was then added. This mixture was incubated at room temperature for 2.5 min, then immediately transferred to ice for 10 min. After 10 min, 1 μ l of mixture was added to 100 μ l of competent *E. coli* DH5 α cells (RBC). DH5 α cells were incubated on ice for 20 min. Then, 950 μ l of LB broth was added and incubated at 37°C for 16 hours. *M. extorquens* AM1 mutants generated by gene-knockout are summarized in Table 1.

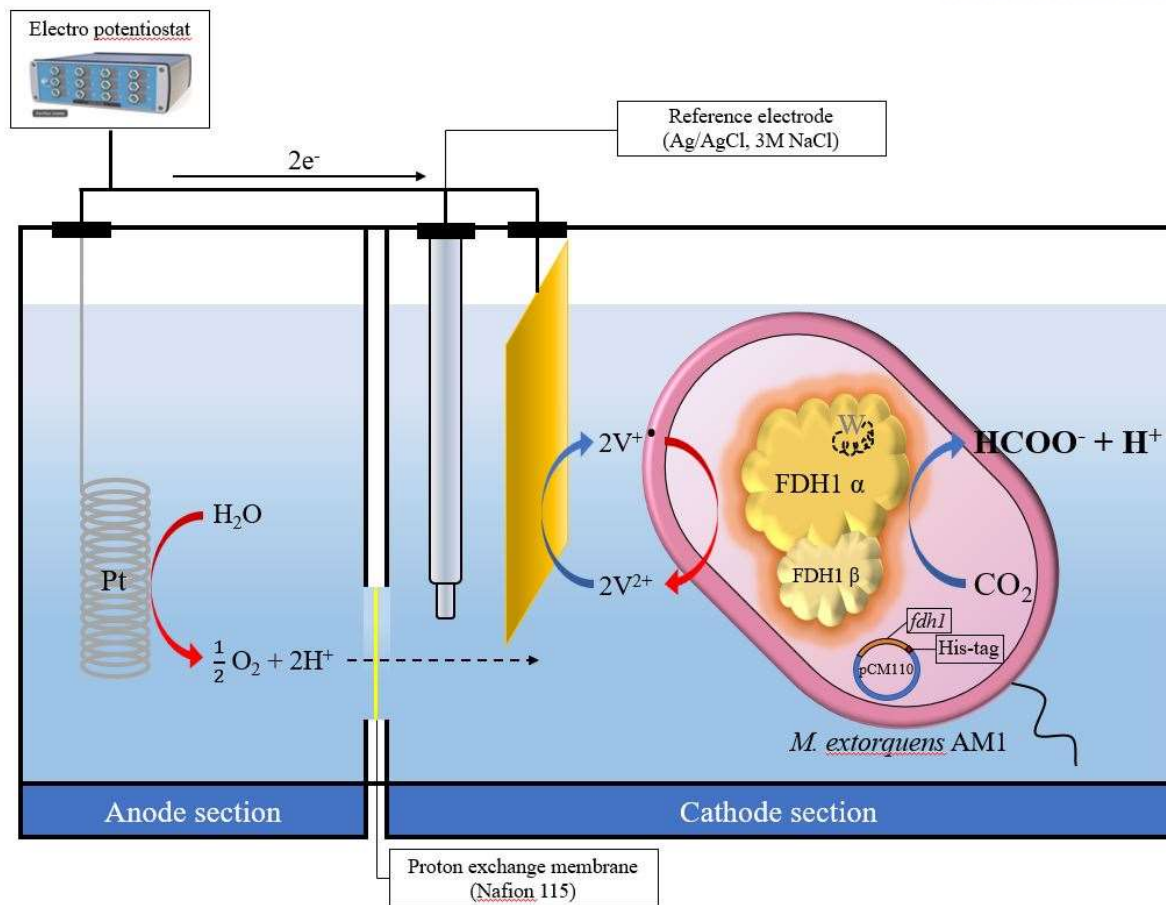
4.3. Western blot analysis for MeFDH1 expression level

Cells were lysed with urea buffer (6 M urea, 200 mM NaCl, 20 mM Tris, pH 8.0) and crude extract was separated on SDS-PAGE (10% Tris/glycine) and transferred to PVDF membrane (Cat. No. KDM20, 10 cm x 10 cm, KOMA BIOTECH) through semi-dry transfer (AE-8130, ATTA) with transfer buffer (24.9 mM Tris, 2.5 M methanol, 191, 8 mM glycine, pH 8.4). After transfer, the membrane was wetted with blocking buffer (PBST; 10 mM phosphate buffer, 2.7 mM KCl, 137 mM NaCl, 1% (w/v) Tween 20) (2% (w/v) skim milk) and was gently shaken for 1 hour. The membrane was washed 4 times for 20 min in PBST buffer and then transferred to blocking buffer mixed with primary antibody and gently shaken for 1 hour. Next, the membrane was washed 4 times for 20 min in PBST buffer and then transferred to blocking buffer mixed with secondary antibody and gently agitated for 1 hour. Finally, the membrane was washed 4 times for 20 min in PBST buffer and then stained with BCIP[□]/NBT Liquid substrate solution (B1911, SIGMA). For the MeFDH1 alpha subunit, the primary antibody was Anti-6x His tag antibody (ab18184, ABCAM) (1:1000 dilution), and the secondary antibody was rabbit anti-mouse (ab6729, ABCAM) (1:2000 dilution). For the MeFDH1 beta subunit, a customized primary antibody was used (ABFRONTIER) (1:1000 dilution) and the secondary antibody was goat anti-rabbit (ab6722, ABCAM) (1:2000 dilution). The intensity of bands in western blot to analyze relative expression level of MeFDH1 was quantified by using Gel-Doc system (Gel-Doc XR system, Bio-Rad).

4.4. Electrochemical CO₂ reduction system and formate analysis

Electrochemical CO₂ reductions were performed as previously reported.¹⁹ The electrochemical reduction system consisted of a copper plate cathode (2 x 1.5 cm), a reference electrode (Ag/AgCl, 3M NaCl), and a platinum wire as anode electrode. During CO₂ reduction reactions, the platinum wire submerged in 1 mM H₂SO₄ aqueous solution (initial volume: 10 mL) and generated both electrons and protons, which passed through a proton-exchange membrane (Nafion 115, 0.005-inch thickness, 30 x 30 cm, Sigma-Aldrich, USA) to the cathode section. The cathode section (initial volume: 10 mL) with 0.6 g of wet-cell as whole-cell biocatalyst, 200 mM potassium phosphate buffer and 10 mM electron mediator (MV or EV) worked to reduce CO₂ to formate by utilizing electrons and protons supplied by the anode section. The cathode section solution was saturated with high purity CO₂ gas (99.999%, purging rate: 1 mL/s) and stirred at 300 rpm at room temperature. When the Ag/AgCl electrode (MF-2079, BASi) was used as reference electrode, the electric potential of redox was constantly controlled by a potentiometer (MultiEnStat3, PalmSens, Netherlands). Scheme 1 is graphical abstract of electrochemical CO₂ reduction system.

The concentration of formate produced by whole-cell catalysis reaction was analyzed with HPLC. HPLC analysis was performed at 30 °C and used a refractive index detector (RID) with an Aminex HPX 87-H Ion Exclusion Column (300 x 7.8 mm, Bio-Rad). The mobile phase was 5 mM H₂SO₄ (0.6 mL/min).



Scheme 1. Graphical abstract of electrochemical CO₂ reduction system.

4.5. MeFDH1 assays and purification

MeFDH1 activity was measured at 30°C by reduction of NAD⁺ (340nm, $\epsilon_{340} = 6220 \text{ M}^{-1} \cdot \text{cm}^{-1}$). The reaction buffer contained 50mM MOPS/KOH (pH 7.0), 30mM sodium formate, 0.5mM NAD⁺ and 20ng of MeFDH1 in final volume of 2.0mL.

MeFDH1 purification used Ni-NTA resin. Cell was suspended in A buffer (50mM MOPS/KOH pH7.0, 20mM imidazole) and sonicated in ice (VCX750, SONICS, USA). Cell debris was removed by centrifugation (12000rpm, 20min, 4°C). The supernatant of cell lysis was flowed through the Ni-NTA column (Ni-NTA Agarose, QIAGEN, Germany). In this step, MeFDH1 containing 6xHis-tag and impurities were bound to the Ni-NTA resin. In washing step, A buffer was flowed through the Ni-NTA column to remove impurities. In final step, B buffer (50mM MOPS/KOH pH7.0, 300mM imidazole) was flowed through the Ni-NTA column for elution of MeFDH1 that was bound to resin. The enzyme concentration was measured using nanodrop (NanoDrop One, Thermo Fisher Scientific, USA).

References

1. Davis, S. J.; Caldeira, K., Consumption-based accounting of CO₂ emissions. *P Natl Acad Sci USA* **2010**, *107* (12), 5687-5692.
2. Solomon, S.; Plattner, G. K.; Knutti, R.; Friedlingstein, P., Irreversible climate change due to carbon dioxide emissions. *Proc Natl Acad Sci U S A* **2009**, *106* (6), 1704-9.
3. Matthews, H. D.; Gillett, N. P.; Stott, P. A.; Zickfeld, K., The proportionality of global warming to cumulative carbon emissions. *Nature* **2009**, *459* (7248), 829-32.
4. Bajracharya, S.; Srikanth, S.; Mohanakrishna, G.; Zacharia, R.; Strik, D. P.; Pant, D., Biotransformation of carbon dioxide in bioelectrochemical systems: State of the art and future prospects. *Journal of Power Sources* **2017**, *356*, 256-273.
5. Bajracharya, S.; Vanbroekhoven, K.; Buisman, C. J. N.; Strik, D.; Pant, D., Bioelectrochemical conversion of CO₂ to chemicals: CO₂ as a next generation feedstock for electricity-driven bioproduction in batch and continuous modes. *Faraday Discuss* **2017**, *202*, 433-449.
6. Aresta, M.; Dibenedetto, A.; Angelini, A., Catalysis for the Valorization of Exhaust Carbon: from CO₂ to Chemicals, Materials, and Fuels. Technological Use of CO₂. *Chem Rev* **2014**, *114* (3), 1709-1742.
7. Otto, A.; Grube, T.; Schiebahn, S.; Stolten, D., Closing the loop: captured CO₂ as a feedstock in the chemical industry. *Energ Environ Sci* **2015**, *8* (11), 3283-3297.
8. Vo, T.; Purohit, K.; Nguyen, C.; Biggs, B.; Mayoral, S.; Haan, J. L., Formate: an Energy Storage and Transport Bridge between Carbon Dioxide and a Formate Fuel Cell in a Single Device. *Chemsuschem* **2015**, *8* (22), 3853-3858.
9. Hellstén, P. P.; Salminen, J. M.; Jørgensen, K. S.; Nystén, T. H., Use of Potassium Formate in Road Winter Deicing Can Reduce Groundwater Deterioration. *Environ Sci Technol* **2005**, *39* (13), 5095-5100.
10. Wang, W.; Wang, S.; Ma, X.; Gong, J., Recent advances in catalytic hydrogenation of carbon dioxide. *Chem Soc Rev* **2011**, *40* (7), 3703-27.
11. Huff, C. A.; Sanford, M. S., Catalytic CO₂ Hydrogenation to Formate by a Ruthenium Pincer Complex. *Acs Catal* **2013**, *3* (10), 2412-2416.
12. Kang, P.; Cheng, C.; Chen, Z.; Schauer, C. K.; Meyer, T. J.; Brookhart, M., Selective electrocatalytic reduction of CO₂ to formate by water-stable iridium dihydride pincer complexes. *J Am Chem Soc* **2012**, *134* (12), 5500-3.
13. Schuchmann, K.; Muller, V., Direct and reversible hydrogenation of CO₂ to formate by a bacterial carbon dioxide reductase. *Science* **2013**, *342* (6164), 1382-5.

14. Bassegoda, A.; Madden, C.; Wakerley, D. W.; Reisner, E.; Hirst, J., Reversible interconversion of CO₂ and formate by a molybdenum-containing formate dehydrogenase. *J Am Chem Soc* **2014**, *136* (44), 15473-6.
15. Nam, D. H.; Kuk, S. K.; Choe, H.; Lee, S.; Ko, J. W.; Son, E. J.; Choi, E.-G.; Kim, Y. H.; Park, C. B., Enzymatic photosynthesis of formate from carbon dioxide coupled with highly efficient photoelectrochemical regeneration of nicotinamide cofactors. *Green Chem* **2016**, *18* (22), 5989-5993.
16. Hollmann, F.; Arends, I. W. C. E.; Holtmann, D., Enzymatic reductions for the chemist. *Green Chem* **2011**, *13* (9).
17. Srikanth, S.; Alvarez-Gallego, Y.; Vanbroekhoven, K.; Pant, D., Enzymatic Electrosynthesis of Formic Acid through Carbon Dioxide Reduction in a Bioelectrochemical System: Effect of Immobilization and Carbonic Anhydrase Addition. *Chemphyschem* **2017**, *18* (22), 3174-3181.
18. Reda, T.; Plugge, C. M.; Abram, N. J.; Hirst, J., Reversible interconversion of carbon dioxide and formate by an electroactive enzyme. *Proc Natl Acad Sci U S A* **2008**, *105* (31), 10654-8.
19. Hwang, H.; Yeon, Y. J.; Lee, S.; Choe, H.; Jang, M. G.; Cho, D. H.; Park, S.; Kim, Y. H., Electro-biocatalytic production of formate from carbon dioxide using an oxygen-stable whole cell biocatalyst. *Bioresour Technol* **2015**, *185*, 35-9.
20. Chistoserdova, L.; Crowther, G. J.; Vorholt, J. A.; Skovran, E.; Portais, J. C.; Lidstrom, M. E., Identification of a fourth formate dehydrogenase in *Methylobacterium extorquens* AM1 and confirmation of the essential role of formate oxidation in methylotrophy. *J Bacteriol* **2007**, *189* (24), 9076-81.
21. Chistoserdova, L.; Laukel, M.; Portais, J. C.; Vorholt, J. A.; Lidstrom, M. E., Multiple Formate Dehydrogenase Enzymes in the Facultative Methylotroph *Methylobacterium extorquens* AM1 Are Dispensable for Growth on Methanol. *J Bacteriol* **2004**, *186* (1), 22-28.
22. Hartmann, T.; Schwanhold, N.; Leimkuhler, S., Assembly and catalysis of molybdenum or tungsten-containing formate dehydrogenases from bacteria. *Biochim Biophys Acta* **2015**, *1854* (9), 1090-100.
23. Lee, S.; Choe, H.; Cho, D. H.; Yoon, S. H.; Won, K.; Kim, Y. H., Communication—Highly Efficient Electroenzymatic NADH Regeneration by an Electron-Relay Flavoenzyme. *J Electrochem Soc* **2016**, *163* (5), G50-G52.
24. Marx, C. J.; Lidstrom, M. E., Development of improved versatile broad-host-range vectors for use in methylotrophs and other Gram-negative bacteria. *Microbiol-Sgm* **2001**, *147*, 2065-2075.
25. Belle, A.; Tanay, A.; Bitincka, L.; Shamir, R.; O'Shea, E. K., Quantification of protein half-lives in the budding yeast proteome. *P Natl Acad Sci USA* **2006**, *103* (35), 13004-13009.

26. Moura, J. J.; Brondino, C. D.; Trincao, J.; Romao, M. J., Mo and W bis-MGD enzymes: nitrate reductases and formate dehydrogenases. *J Biol Inorg Chem* **2004**, *9* (7), 791-9.
27. Zhang, Y.; Gladyshev, V. N., Molybdoproteomes and evolution of molybdenum utilization. *J Mol Biol* **2008**, *379* (4), 881-99.
28. Girio, F. M.; Roseiro, J. C.; Silva, A. I., The effect of the simultaneous addition of molybdenum and tungsten to the culture medium on the formate dehydrogenase activity from *Methylobacterium* sp. RXM. *Curr Microbiol* **1998**, *36* (6), 337-340.
29. Marx, C. J.; Chistoserdova, L.; Lidstrom, M. E., Formaldehyde-Detoxifying Role of the Tetrahydromethanopterin-Linked Pathway in *Methylobacterium extorquens* AM1. *J Bacteriol* **2003**, *185* (24), 7160-7168.
30. Gírio, F. M.; Marcos, J. C.; Amaral-Collação, M. T., Transition metal requirement to express high level NAD⁺-dependent formate dehydrogenase from a serine-type methylotrophic bacterium. *Fems Microbiol Lett* **1992**, *97* (1), 161-166.
31. Sakai, K.; Hsieh, B.-C.; Maruyama, A.; Kitazumi, Y.; Shirai, O.; Kano, K., Interconversion between formate and hydrogen carbonate by tungsten-containing formate dehydrogenase-catalyzed mediated bioelectrocatalysis. *Sensing and Bio-Sensing Research* **2015**, *5*, 90-96.
32. Sakai, K.; Kitazumi, Y.; Shirai, O.; Kano, K., Bioelectrocatalytic formate oxidation and carbon dioxide reduction at high current density and low overpotential with tungsten-containing formate dehydrogenase and mediators. *Electrochemistry Communications* **2016**, *65*, 31-34.
33. Espirito Santo, C.; Taudte, N.; Nies, D. H.; Grass, G., Contribution of copper ion resistance to survival of *Escherichia coli* on metallic copper surfaces. *Appl Environ Microbiol* **2008**, *74* (4), 977-86.
34. Ochoa-Herrera, V.; Leon, G.; Banihani, Q.; Field, J. A.; Sierra-Alvarez, R., Toxicity of copper(II) ions to microorganisms in biological wastewater treatment systems. *Sci Total Environ* **2011**, *412-413*, 380-5.
35. Benedetti, T. M.; Carvalho, T.; Iwakura, D. C.; Braga, F.; Vieira, B. R.; Vidinha, P.; Gruber, J.; Torresi, R. M., All solid-state electrochromic device consisting of a water soluble viologen dissolved in gelatin-based ionogel. *Solar Energy Materials and Solar Cells* **2015**, *132*, 101-106.
36. Park, Y. S.; Lee, K.; Lee, C.; Yoon, K. B., Facile Reduction of Zeolite-Encapsulated Viologens with Solvated Electrons and Selective Dispersion of Inter- and Intramolecular Dimers of Propylene-Bridged Bisviologen Radical Cation. *Langmuir* **2000**, *16* (10), 4470-4477.
37. Marx, C. J.; Lidstrom, M. E., Broad-host-range cre-lox system for antibiotic marker recycling in gram-negative bacteria. *Biotechniques* **2002**, *33* (5), 1062-1067.

38. Jeong, J. Y.; Yim, H. S.; Ryu, J. Y.; Lee, H. S.; Lee, J. H.; Seen, D. S.; Kang, S. G., One-step sequence- and ligation-independent cloning as a rapid and versatile cloning method for functional genomics studies. *Appl Environ Microbiol* **2012**, *78* (15), 5440-3.